Inorg. Chem. **2009**, *48*, 296−306

Accessing Postsynthetic Modification in a Series of Metal-Organic Frameworks and the Influence of Framework Topology on Reactivity

Zhenqiang Wang, Kristine K. Tanabe, and Seth M. Cohen*

Department of Chemistry and Biochemistry, University of California, San Diego, 9500 Gilman Drive, La Jolla, California 92093-0358

Received September 25, 2008

2-Amino-1,4-benzenedicarboxylic acid (NH_2−BDC) has been found to be a compatible building block for the construction of two new metal-organic frameworks (MOFs) that have structures isoreticular to reported MOFs that use 1,4-benzenedicarboxylic acid (BDC) as a building block. DMOF-1-NH_2 (DABCO MOF-1-NH_2) is a derivative of a previously studied MOF that contains two-dimensional square grids based on NH_2−BDC and zinc(II) paddlewheel units; the grid layers are connected by DABCO (1,4-diazabicyclo[2.2.2]octane) molecules that coordinate in the axial positions of the paddlewheel secondary-building units (SBUs). UMCM-1-NH_2 is an NH_2−BDC derivative of UMCM-1 (University of Michigan Crystalline Material-1), a highly porous MOF reported by Matzger et al., and consists of both NH_2−BDC and BTB (BTB = 4,4′,4″-benzene-1,3,5-triyl-tribenzoate) linkers with Zn_4O SBUs. The structure of UMCM-1-NH_2 was confirmed by single-crystal X-ray diffraction. By using NH_2−BDC to generate these MOFs, the pendant amino groups can serve as a chemical handle that can be manipulated via postsynthetic modification with alkyl anhydrides. Reactions of each MOF and different anhydrides have been performed to compare the extent of conversion, thermal and structural stability, and Brunauer−Emmett−Teller surface areas afforded by the resulting materials. Under comparable reaction conditions, ^{1}H NMR of digested samples show that UMCM-1-NH_2 has conversions comparable to that of IRMOF-3, while DMOF-1-NH_2 only shows high conversions with smaller anhydrides. Under specific reaction conditions, higher conversions were obtained with complete retention of crystallinity, as verified by single-crystal X-ray diffraction experiments. The results presented here demonstrate three important findings: (a) NH_2−BDC can be used as a surrogate for BDC in a number of MOFs thereby providing a handle for postsynthetic modification, (b) postsynthetic modification is a general strategy to functionalizing MOFs that can be applied to a variety of MOF structures, and (c) the topology and chemical/thermal stability of a MOF can influence the type of chemical reactions and reagents that can be used for postsynthetic modification.

Introduction

Metal-organic frameworks (MOFs) are porous crystalline materials composed of metal ions or metal ion clusters which are linked together by multidentate organic ligands.[1−16] Numerous combinations of metals and ligands have resulted in the synthesis of many MOFs with different structures and topologies. MOFs are characteristically known for exhibiting high porosities and good thermal stability, and some MOFs

* To whom correspondence should be addressed. E-mail: scohen@ucsd.edu. Phone: (858) 822-5596. Fax: (858) 822-5598.

(1) Hoskins, B. F.; Robson, R. *J. Am. Chem. Soc.* **1989**, *111*, 5962–5964.
(2) Hoskins, B. F.; Robson, R. *J. Am. Chem. Soc.* **1990**, *112*, 1546–1554.
(3) Gardner, G. B.; Venkataraman, D.; Moore, J. S.; Lee, S. *Nature* **1995**, *374*, 792–795.
(4) Yaghi, O. M.; Li, H. L.; Davis, C.; Richardson, D.; Groy, T. L. *Acc. Chem. Res.* **1998**, *31*, 474–484.
(5) Kitagawa, S.; Kondo, M. *Bull. Chem. Soc. Jpn.* **1998**, *71*, 1739–1753.
(6) Robson, R. *J. Chem. Soc., Dalton Trans.* **2000**, 3735–3744.
(7) Eddaoudi, M.; Moler, D. B.; Li, H.; Chen, B.; Reineke, T. M.; O'Keeffe, M.; Yaghi, O. M. *Acc. Chem. Res.* **2001**, *34*, 319–330.
(8) Moulton, B.; Zaworotko, M. J. *Chem. Rev.* **2001**, *101*, 1629–1658.
(9) Janiak, C. *Dalton Trans.* **2003**, 2781–2804.
(10) James, S. L. *Chem. Soc. Rev.* **2003**, *32*, 276–288.
(11) Yaghi, O. M.; O'Keeffe, M.; Ockwig, N. W.; Chae, H. K.; Eddaoudi, M.; Kim, J. *Nature* **2003**, *423*, 705–714.
(12) Kitagawa, S.; Kitaura, R.; Noro, S.-i. *Angew. Chem., Int. Ed.* **2004**, *43*, 2334–2375.
(13) Rao, C. N. R.; Natarajan, S.; Vaidhyanathan, R. *Angew. Chem., Int. Ed.* **2004**, *43*, 1466–1496.
(14) Ockwig, N. W.; Delgado-Friedrichs, O.; O'Keeffe, M.; Yaghi, O. M. *Acc. Chem. Res.* **2005**, *38*, 176–182.
(15) Férey, G.; Mellot-Draznieks, C.; Serre, C.; Millange, F. *Acc. Chem. Res.* **2005**, *38*, 217–225.
(16) Bradshaw, D.; Claridge, J. B.; Cussen, E. J.; Prior, T. J.; Rosseinsky, M. J. *Acc. Chem. Res.* **2005**, *38*, 273–282.

10.1021/ic801837t CCC: $40.75 © 2009 American Chemical Society
Published on Web 11/20/2008

have been explored for applications such as gas storage, catalysis, and separations.[12,17−38] Interest in the aforementioned uses has resulted in a rational, designed approach in the preparation of MOFs, where the choice of metal ion and ligand can be judiciously selected to influence the overall chemical and physical properties of the MOF.[39−44] Although the ability to incorporate "functional" metal centers into MOFs (e.g., unsaturated metal centers) has improved,[45−47] the introduction of ligands containing complex functional groups into the MOF has faced greater challenges because of the reactivity of such groups with metal ions, particularly under solvothermal conditions.

As an alternative route, we adapted a concept from Robson et al.,[2] which had been previously validated by Kim and coworkers,[29] whereby we first synthesized a MOF and then functionalized the lattice afterward using suitable chemical reagents. To describe this approach for functionalizing MOFs, the phrase "postsynthetic modification" was adopted, in reference to the process of posttranslational modification of proteins.[48] Postsynthetic modification has been demonstrated with other solid state materials (e.g., organosilicates,[49,50] carbon nanotubes[51]) but is a relatively new concept in the field of MOFs.[29,34,52−56] Recently, we[57−60] and others[61−67] were able to demonstrate the feasibility of using postsynthetic modification to decorate MOFs with a variety of functional groups. For example, isoreticular metal-organic framework-3 (IRMOF-3),[68] which is composed of 2-amino-1,4-benzenedicarboxylic acid (NH_2−BDC) and Zn_4O clusters, can readily be modified with linear alkyl chain anhydrides[57,59] and isocyanates[60] to produce amide and urea functionalized systems. It has been shown that these modifications can affect the physical and chemical properties of IRMOF-3, including its microporosity.

Despite the impressive progress that has been made in the postsynthetic functionalization of MOFs, there appear to exist a number of important issues that need to be further addressed. First, approaches that can provide general and facile access to covalent modification of different MOFs are currently not available. Second, although the effect of reagent *size* on the outcome of IRMOF-3 modification has been probed,[59] it remains unclear how reagent *shape* (e.g., linear vs branched) might influence the process of postsynthetic

(17) Rosi, N. L.; Eckert, J.; Eddaoudi, M.; Vodak, D. T.; Kim, J.; O'Keeffe, M.; Yaghi, O. M. *Science* **2003**, *300*, 1127–1129.
(18) Férey, G.; Latroche, M.; Serre, C.; Millange, F.; Loiseau, T.; Percheron-Guégan, A. *Chem. Commun.* **2003**, 2976–2977.
(19) Rowsell, J. L. C.; Millward, A. R.; Park, K. S.; Yaghi, O. M. *J. Am. Chem. Soc.* **2004**, *126*, 5666–5667.
(20) Rowsell, J. L. C.; Yaghi, O. M. *Angew. Chem., Int. Ed.* **2005**, *44*, 4670–4679.
(21) Eddaoudi, M.; Kim, J.; Rosi, N.; Vodak, D.; Wachter, J.; O'Keeffe, M.; Yaghi, O. M. *Science* **2002**, *295*, 469–472.
(22) Ma, S.; Sun, D.; Simmons, J. M.; Collier, C. D.; Yuan, D.; Zhou, H.-C. *J. Am. Chem. Soc.* **2008**, *130*, 1012–1016.
(23) Matsuda, R.; Kitaura, R.; Kitagawa, S.; Kubota, Y.; Belosludov, R. V.; Kobayashi, T. C.; Sakamoto, H.; Chiba, T.; Takata, M.; Kawazoe, Y.; Mita, Y. *Nature* **2005**, *436*, 238–241.
(24) Millward, A. R.; Yaghi, O. M. *J. Am. Chem. Soc.* **2005**, *127*, 17998–17999.
(25) Banerjee, R.; Phan, A.; Wang, B.; Knobler, C.; Furukawa, H.; O'Keeffe, M.; Yaghi, O. M. *Science* **2008**, *319*, 939–943.
(26) Fujita, M.; Kwon, Y. J.; Washizu, S.; Ogura, K. *J. Am. Chem. Soc.* **1994**, *116*, 1151–1152.
(27) Li, H.; Eddaoudi, M.; O'Keeffe, M.; Yaghi, O. M. *Nature* **1999**, *402*, 276–279.
(28) Chui, S. S.-Y.; Lo, S. M.-F.; Charmant, J. P. H.; Orpen, A. G.; Williams, I. D. *Science* **1999**, *283*, 1148–1150.
(29) Seo, J. S.; Whang, D.; Lee, H.; Jun, S. I.; Oh, J.; Jeon, Y. J.; Kim, K. *Nature* **2000**, *404*, 982–986.
(30) Halder, G. J.; Kepert, C. J.; Moubaraki, B.; Murray, K. S.; Cashion, J. D. *Science* **2002**, *298*, 1762–1765.
(31) Chae, H. K.; Siberio-Pérez, D. Y.; Kim, J.; Go, Y.; Eddaoudi, M.; Matzger, A. J.; O'Keeffe, M.; Yaghi, O. M. *Nature* **2004**, *427*, 523–527.
(32) Férey, G.; Mellot-Draznieks, C.; Serre, C.; Millange, F.; Dutour, J.; Surblé, S.; Margiolaki, I. *Science* **2005**, *309*, 2040–2042.
(33) Evans, O. R.; Lin, W. B. *Acc. Chem. Res.* **2002**, *35*, 511–522.
(34) Wu, C.-D.; Hu, A.; Zhang, L.; Lin, W. *J. Am. Chem. Soc.* **2005**, *127*, 8940–8941.
(35) Lin, W. B. *J. Solid State Chem.* **2005**, *178*, 2486–2490.
(36) Cho, S.-H.; Ma, B.; Nguyen, S. T.; Hupp, J. T.; Albrecht-Schmitt, T. E. *Chem. Commun.* **2006**, 2563–2565.
(37) Nuzhdin, A. L.; Dybtsev, D. N.; Bryliakov, K. P.; Talsi, E. P.; Fedin, V. P. *J. Am. Chem. Soc.* **2007**, *129*, 12958–12959.
(38) Mueller, U.; Schubert, M.; Teich, F.; Puetter, H.; Schierle-Arndt, K.; Pastré, J. *J. Mater. Chem.* **2006**, *16*, 626–636.
(39) Custelcean, R.; Gorbunova, M. G. *J. Am. Chem. Soc.* **2005**, *127*, 16362–16363.
(40) Kawano, M.; Kawamichi, T.; Haneda, T.; Kojima, T.; Fujita, M. *J. Am. Chem. Soc.* **2007**, *129*, 15418–15419.
(41) Oh, M.; Carpenter, G. B.; Sweigart, D. A. *Acc. Chem. Res.* **2004**, *37*, 1–11.
(42) Kitagawa, S.; Noro, S.-i.; Nakamura, T. *Chem. Commun.* **2006**, *70*, 1–707.
(43) Halper, S. R.; Do, L.; Stork, J. R.; Cohen, S. M. *J. Am. Chem. Soc.* **2006**, *128*, 15255–15268.
(44) Kitaura, R.; Onoyama, G.; Sakamoto, H.; Matsuda, R.; Noro, S.-i.; Kitagawa, S. *Angew. Chem., Int. Ed.* **2004**, *43*, 2684–2687.
(45) Ma, S.; Zhou, H.-C. *J. Am. Chem. Soc.* **2006**, *128*, 11734–11735.
(46) Forster, P. M.; Eckert, J.; Heiken, B. D.; Parise, J. B.; Yoon, J. W.; Jhung, S. H.; Chang, J.-S.; Cheetham, A. K. *J. Am. Chem. Soc.* **2006**, *128*, 16846–16850.
(47) Dinca, M.; Dailly, A.; Liu, Y.; Brown, C. M.; Neumann, D. A.; Long, J. R. *J. Am. Chem. Soc.* **2006**, *128*, 16876–16883.
(48) Walsh, C. T.; Garneau-Tsodikova, S.; Gatto, G. J., Jr. *Angew. Chem., Int. Ed.* **2005**, *44*, 7342–7372.
(49) Inagaki, S.; Guan, S.; Ohsuna, T.; Terasaki, O. *Nature* **2002**, *416*, 304–307.
(50) Yang, Q.; Kapoor, M. P.; Inagaki, S. *J. Am. Chem. Soc.* **2002**, *124*, 9694–9695.
(51) Hirsch, A. *Angew. Chem., Int. Ed.* **2002**, *41*, 1853–1859.
(52) Kiang, Y.-H.; Gardner, G. B.; Lee, S.; Xu, Z.; Lobkovsky, E. B. *J. Am. Chem. Soc.* **1999**, *121*, 8204–8215.
(53) Xu, Z.; Lee, S.; Kiang, Y.-H.; Mallik, A. B.; Tsomaia, N.; Mueller, K. T. *Adv. Mater.* **2001**, *13*, 637–641.
(54) Wang, X.-S.; Ma, S.; Sun, D.; Parkin, S.; Zhou, H.-C. *J. Am. Chem. Soc.* **2006**, *128*, 16474–16475.
(55) Mulfort, K. L.; Hupp, J. T. *J. Am. Chem. Soc.* **2007**, *129*, 9604–9605.
(56) Choi, H. J.; Suh, M. P. *J. Am. Chem. Soc.* **2004**, *126*, 15844–15851.
(57) Wang, Z.; Cohen, S. M. *J. Am. Chem. Soc.* **2007**, *129*, 12368–12369.
(58) Wang, Z.; Cohen, S. M. *Angew. Chem., Int. Ed.* **2008**, *47*, 4699–4702.
(59) Tanabe, K. K.; Wang, Z.; Cohen, S. M. *J. Am. Chem. Soc.* **2008**, *130*, 8508–8517.
(60) Dugan, E.; Wang, Z.; Okamura, M.; Medina, A.; Cohen, S. M. *Chem. Commun.* **2008**, 3366–3368.
(61) Haneda, T.; Kawano, M.; Kawamichi, T.; Fujita, M. *J. Am. Chem. Soc.* **2008**, *130*, 1578–1579.
(62) Kaye, S. S.; Long, J. R. *J. Am. Chem. Soc.* **2008**, *130*, 806–807.
(63) Ingleson, M. J.; Barrio, J. P.; Bacsa, J.; Dickinson, C.; Park, H.; Rosseinsky, M. J. *Chem. Commun.* **2008**, 1287–1289.
(64) Costa, J. S.; Gamez, P.; Black, C. A.; Roubeau, O.; Teat, S. J.; Reedijk, J. *Eur. J. Inorg. Chem.* **2008**, 1551–1554.
(65) Ingleson, M. J.; Barrio, J. P.; Guilbaud, J. B.; Khimyak, Y. Z.; Rosseinsky, M. J. *Chem Commun* **2008**, 2680–2682.
(66) Horike, S.; Dinca, M.; Tamaki, K.; Long, J. R. *J. Am. Chem. Soc.* **2008**, *130*, 5854–5855.
(67) Hwang, Y. K.; Hong, D. Y.; Chang, J. S.; Jhung, S. H.; Seo, Y. K.; Kim, J.; Vimont, A.; Daturi, M.; Serre, C.; Ferey, G. *Angew. Chem., Int. Ed.* **2008**, *47*, 4144–4148.
(68) Rowsell, J. L. C.; Yaghi, O. M. *J. Am. Chem. Soc.* **2006**, *128*, 1304–1315.

Scheme 1. Synthesis and Postsynthetic Modification of Three MOFs: DMOF-1-NH_2, IRMOF-3, and UMCM-1-NH_2[a]

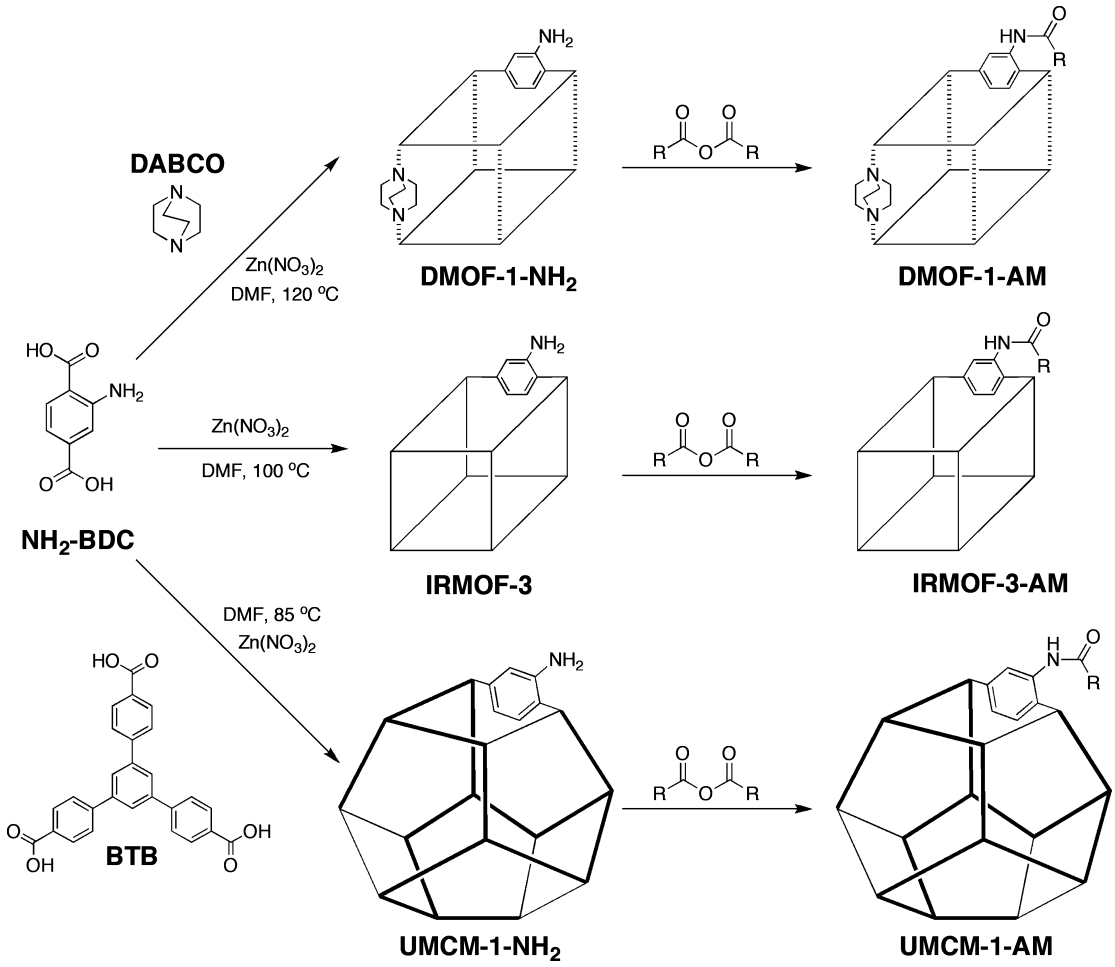

[a] DABCO and BTB ligands are represented by dashed and bold lines in the scheme, respectively.

modification. Similarly, MOFs with different pore sizes and topologies could also potentially have variable postsynthetic modification outcomes, even when treated with the same reagents under identical conditions. Furthermore, there are a very limited number of literature reports on the postsynthetic modification of MOFs, and hence exploring the generality of postsynthetic modification with a variety of MOF structures is also an unrealized and important goal. Although the postsynthetic modification of MOFs other than IRMOF-3 has been performed,[29,61,64,65] none of these studies report a systematic investigation of postsynthetic modification as a function of reagent size and reactivity. To gain a better understanding of the relationship between postsynthetic modification and topology, and examine other fundamental aspects of this relatively new field, we sought to design MOFs specifically for postsynthetic modification. On the basis of the work performed with IRMOF-3, which had proven to be a successful model system because of its combination of high porosity, good crystallinity, and uncoordinated amino groups, NH_2−BDC was selected as a surrogate for 1,4-benzenedicarboxylate (BDC) to synthesize MOFs amenable to postsynthetic modification. In this way, the same functional unit could be used to explore the postsynthetic modification of different MOFs, allowing for similarities and differences observed in reactivity to be attributed to MOF topology and structure.

In the present study, we describe two new MOFs (designated DMOF-1-NH_2 and UMCM-1-NH_2) that have been synthesized using NH_2−BDC, which can be modified by postsynthetic modification (Scheme 1). The two new MOFs are derivatives of previously reported structures, where NH_2−BDC was substituted for BDC under solvothermal conditions.[69−71] Both MOFs and IRMOF-3 were modified with linear alkyl chain anhydrides ($[CH_3(CH_2)_nCO]_2O$, where $n = 0, 2, 4, 8, 12, 18$) and branched anhydrides (trimethylacetic anhydride and isobutyric anhydride). The degree of modification was probed by solution ^1H NMR, and the modifications were confirmed by Electrospray Ionization Mass Spectrometry (ESI-MS). Thermal and structural stability of the modified MOFs were examined using thermogravimetric analysis (TGA), powder X-ray diffraction (PXRD), and single-crystal X-ray analysis. Brunauer−Emmett−Teller

(69) Dybtsev, D. N.; Chun, H.; Kim, K. *Angew. Chem., Int. Ed.* **2004**, *43*, 5033–5036.
(70) Lee, J. Y.; Olson, D. H.; Pan, L.; Emge, T. J.; Li, J. *Adv. Funct. Mat.* **2007**, *17*, 1255–1262.
(71) Koh, K.; Wong-Foy, A. G.; Matzger, A. J. *Angew. Chem., Int. Ed.* **2008**, *47*, 677–680.

(BET) surface areas of the MOFs were also determined using N_2 isotherms at 77 K to examine the porosity of the modified materials. DMOF-1-NH_2 and UMCM-1-NH_2 showed similar trends in the degree of conversion, with modification decreasing as the alkyl chain length increased. All of the MOFs demonstrated little or no modification with trimethylacetic anhydride. Postsynthetic modification of the MOFs was influenced by the accessibility and probable orientation of the NH_2−BDC within the framework. The results here demonstrate the versatility of using NH_2−BDC for synthesizing new MOFs, highlight differences in the postsynthetic modification as a function of MOF structure, and show that covalent postsynthetic modification is a broadly applicable approach to the functionalization of MOFs.

Experimental Methods

Starting materials and solvents were purchased and used without further purification from commercial suppliers (Sigma-Aldrich, Alfa Aesar, EMD, TCI, Cambridge Isotope Laboratories, Inc., and others). IRMOF-3 was synthesized and activated as described previously.[59,72]

Preparation of DMOF-1-NH_2. $Zn(NO_3)_2 \cdot 4H_2O$ (1.56 g, 6.00 mmol) and 2-amino-1,4-benzenedicarboxylic acid (NH_2−BDC, 1.10 g, 6.07 mmol) were dissolved in 150 mL of dimethylformamide (DMF). 1,4-Diazabicyclo[2.2.2]octane (DABCO, 1.08 g, 9.63 mmol) was then added to the solution, which immediately generated a large amount of white precipitate. The mixture was filtered using a 60 mL PYREX glass funnel of fine porosity. The filtrate was collected, and the solution was diluted to a volume of 150 mL with DMF before being divided into 15 mL portions and transferred to 10 scintillation vials (20 mL capacity each). The vials were placed in a sand bath, and the bath was transferred to a programmable oven and heated at a rate of 2.5 °C/min from 35 to 120 °C. The temperature was held at 120 °C for 12 h, and then the oven was cooled at a rate of 2.5 °C/min to a final temperature of 35 °C. This procedure generated yellowish rod-shaped crystals of DMOF-1-NH_2. The mother liquor from each vial was decanted, and the crystals were washed with 3 × 6 mL of DMF followed by 3 × 6 mL of $CHCl_3$. The crystals were then soaked in 10 mL of $CHCl_3$ for 3 days with fresh $CHCl_3$ added every 24 h. After 3 days of soaking the crystals were stored in the last $CHCl_3$ solution until needed. The average yield of dried DMOF-1-NH_2 per vial was determined to be approximately 57 ± 3 mg (0.20 mmol −NH_2 equiv., 33% based on starting $Zn(NO_3)_2 \cdot 4H_2O$). Substituting NH_2−BDC with BDC (1.02 g, 0.60 mmol) using an identical procedure led to the generation of DMOF-1 crystals.[69,70]

Preparation of UMCM-1-NH_2. $Zn(NO_3)_2 \cdot 4H_2O$ (2.83 g, 10.8 mmol), NH_2−BDC (0.490 g, 2.7 mmol), and 4,4′,4″-benzene-1,3,5-triyl-tribenzoic acid[75] (BTB, 0.424 g, 0.97 mmol) were dissolved in 100 mL of DMF. The solution was divided into 10 mL portions and transferred to 10 scintillation vials (20 mL capacity each). The vials were placed in a sand bath, and the bath was transferred to an isothermal oven heated at 85 °C. After 48 h, the vials were removed from the oven and left to cool to room temperature. Beige, crystalline needle clusters were present in every vial. The mother liquor was decanted, and crystals were washed with 3 × 12 mL of DMF and soaked in $CHCl_3$ (12 mL) for 24 h. The crystals were then rinsed 3 × 10 mL of $CHCl_3$ and left to soak for 3 days with fresh $CHCl_3$ added every 24 h. After 3 days of soaking the crystals were stored in the last $CHCl_3$ solution until needed. The average yield of dried UMCM-1-NH_2 per vial was determined to be approximately 56 mg (0.05mmol -NH_2 equiv, ∼56% based on BTB).

Modification of MOFs − Method 1. The $CHCl_3$ storage solution of each MOF was decanted, and the crystals were dried at 75 °C under vacuum for at least 12 h. The freshly dried MOF sample (∼15 mg, 0.050 mmol equiv of -NH_2 of DMOF-1-NH_2; 52 mg, 0.050 mmol equiv of -NH_2 of UMCM-1-NH_2; 14 mg, 0.050 mmol equiv of -NH_2 of IRMOF-3) was placed into a dram vial (4 mL capacity) with 1.0 mL of solvent ($CDCl_3$ or $CHCl_3$) and 2 equiv (0.10 mmol) of anhydride. The samples were left to react for 3 days at room temperature, and the reaction was quenched by decanting the solvent. The samples were rinsed with 3 × 2 mL of $CHCl_3$ and soaked in 2 mL of $CHCl_3$ overnight. The rinsing and soaking were repeated for a total of 3 days, and the samples were left in fresh $CHCl_3$. Each vial was dried under vacuum at room temperature or at 90 °C overnight and used for ^{1}H NMR analysis.

Modification of MOFs − Method 2. For DMOF-1-NH_2: Approximately 57 mg of DMOF-1-NH_2 (0.20 mmol, equiv of -NH_2) was placed in a vial with 2 equiv (0.4 mmol) of alkyl anhydride dissolved in either 8 mL (for $n = 0$, 2) or 4 mL (for $n = 4$, 8, 12, 18; isobutyric anhydride, trimethylacetic anhydride) of $CHCl_3$. The samples were heated in an oven at 55 °C for 24 h, after which the solution was decanted (except for $n = 12$ and 18, vide infra) and the crystals were washed with 3 × 6 mL of $CHCl_3$. A fresh solution of the anhydride was added to the vial, and the mixtures were heated for an additional 24 h. The aforementioned procedure was repeated two more times, giving a total reaction time of 4 days. For samples where $n = 12$ or 18, the mixtures were heated at 55 °C for 4 days without replacing the anhydride solution, but the volume was adjusted to 4 mL every 24 h by adding fresh $CHCl_3$ (some solvent loss occurred because of evaporation). After the reaction was complete, the $CHCl_3$ solution was decanted, and the crystals were washed with 3 × 6 mL of $CHCl_3$ before soaking in 10 mL of pure $CHCl_3$ (i.e., without anhydride) for 3 days, with fresh $CHCl_3$ added every 24 h. After 3 days of soaking the crystals were stored in the last $CHCl_3$ solution until analyzed.

For UMCM-1-NH_2: One vial of UMCM-1-NH_2 (∼56 mg, ca. 0.050 mmol equiv of -NH_2) was combined with 4 equiv (0.20 mmol for $n = 0$, 18) or 8 equiv (0.40 mmol for $n = 2$, 4, 8, 12, isobutyric anhydride, trimethylacetic anhydride) of alkyl anhydride in 2 mL of $CHCl_3$. The reduced equivalents/concentration (0.1 M vs 0.2 M) used for $n = 0$ and $n = 18$ were due to the high reactivity ($n = 0$) and low solubility ($n = 18$) of these anhydrides. After allowing the sample to stand at room temperature for 3 days, the solution was decanted, and the crystals were washed with 3 × 10 mL of $CHCl_3$ before soaking in 10 mL of $CHCl_3$ for 24 h. After repeating the washes and soaks for 3 days, the crystals were stored in the last $CHCl_3$ solution until analyzed.

Digestion and Analysis by ^{1}H NMR. ^{1}H NMR spectra were recorded on Varian FT-NMR spectrometer (400 MHz). Approximately 5 mg of MOF (DMOF-1-NH_2, UMCM-1-NH_2, or IRMOF-3) modified using either Method 1 or Method 2 was dried under vacuum at room temperature or at 90 °C overnight and

(72) Rowsell, J. L.; Yaghi, O. M. *J. Am. Chem. Soc.* **2006**, *128*, 1304–1315.
(73) Takei, T.; Kawashima, J.; Ii, T.; Maeda, A.; Hasegawa, M.; Kitagawa, T.; Ohmura, T.; Ichikawa, M.; Hosoe, M.; Kanoya, I.; Mori, W. *Bull. Chem. Soc. Jpn.* **2008**, *81*, 847–856.
(74) Arstad, B.; Fjellvåg, H.; Kongshaug, K. O.; Swang, O.; Blom, R. *Adsorption* **2008**, *14*, 755–762.
(75) Choi, S. B.; Seo, M. J.; Cho, M.; Kim, Y.; Jin, M. K.; Jung, D.-Y.; Choi, J.-S.; Ahn, W.-S.; Rowsell, J. L. C.; Kim, J. *Cryst. Growth Des.* **2007**, *7*, 2290–2293.

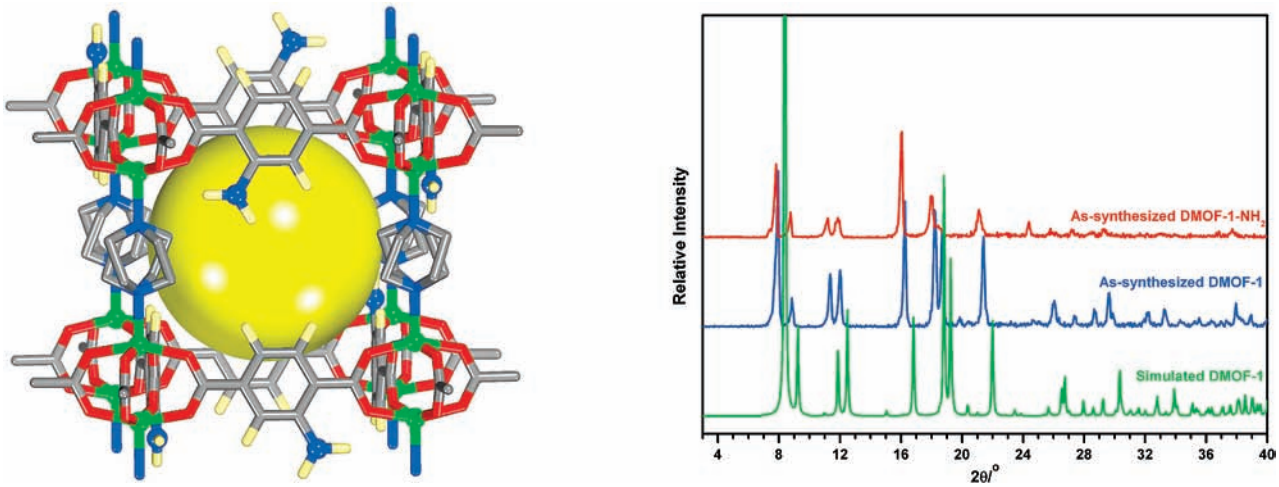

Figure 1. Proposed structural model for DMOF-1-NH_2 (left), based on the reported structure of DMOF-1. Color scheme: green, Zn; red, O; gray, C; blue, N; gold, H. DABCO molecules are shown with disorder as reported for DMOF-1. The yellow sphere illustrates estimated free space. PXRD (right) of the as-synthesized DMOF-1-NH_2 (red), as-synthesized DMOF-1 (blue), and simulated DMOF-1 (green) derived from ref 70.

digested with sonication in 500 μL of DMSO-d_6 and 100 μL of dilute DCl (23 μL of 35% DCl in D_2O diluted with 1.0 mL of DMSO-d_6).

Digestion and Analysis by ESI-MS. ESI-MS was performed using a ThermoFinnigan LCQ-DECA mass spectrometer, and the data was analyzed using the Xcalibur software suite. Crystals of modified DMOF-1-NH_2 and UMCM-1-NH_2 (0.1∼1 mg) were digested in 1 mL of MeOH (or H_2O) with sonication.

Thermal Analysis. Approximately 10−20 mg of IRMOF-3, DMOF-1-NH_2, or UMCM-1-NH_2 modified using Method 2 was used for TGA measurements. Samples were analyzed under a stream of dinitrogen using a TA Instrument Q600 SDT running from room temperature to 600 °C with a scan rate of 5 °C/min.

PXRD Analysis. Approximately 15 mg of DMOF-1-NH_2 (typically soaked in DMF) or UMCM-1-NH_2 (typically soaked in $CHCl_3$) modified using Method 2 were air-dried before PXRD analysis. PXRD data were collected at ambient temperature on a Rigaku Miniflex II diffractometer at 30 kV, 15 mA for Cu Kα (λ = 1.5418 Å), with a scan speed of 1°/min or 5°/min, a step size of 0.05° in 2θ, and a 2θ range of 3−40° and 2−35° for DMOF-1-NH_2 samples and UMCM-1-NH_2 samples, respectively. The experimental backgrounds were corrected using the Jade 5.0 software package. The simulated PXRD patterns were calculated from the single crystal diffraction data using Mercury CSD 2.0.

BET Surface Area Analysis. Approximately 80−100 mg of modified DMOF-1-NH_2 or 40−60 mg of modified UMCM-1-NH_2 (prepared using Method 2) was evacuated on a vacuum line for 5−18 h. The sample was then transferred to a preweighed sample tube and degassed at 105 °C for approximately 24 h on an ASAP 2020 or until the outgas rate was <5 μm Hg/min. The sample tube was reweighed to obtain a consistent mass for the degassed modified DMOF-1-NH_2 or UMCM-1-NH_2. BET surface area (m^2/g) measurements were collected at 77 K by dinitrogen on an ASAP 2020 using volumetric technique.

Single-Crystal X-ray Diffraction. Single crystals of UMCM-1-NH_2 and UMCM-1-AM5 in $CHCl_3$ were mounted on nylon loops with Paratone oil and placed under a nitrogen cold stream (200 K). Data was collected on a Bruker Kappa Apex II diffractometer using Cu Kα radiation (λ = 1.54178 Å) controlled using the APEX 2.0 software package. A semiempirical method utilizing equivalents was employed to correct for absorption. All data collections were solved and refined using the SHELXTL suite. The Zn^{2+} ions, O atoms, and several of the C atoms were refined anisotropically while the rest of the C atoms were refined isotropically for UMCM-1-NH_2. All non-hydrogen atoms, except for atoms C3 and C4, were refined anisotropically for UMCM-1-AM5. UMCM-1-NH_2 and UMCM-1-AM5 were treated with the "squeeze" protocol in PLATON to account for electron density associated with the amino and alkyl-amide substituents and for partially occupied or disordered solvent (e.g., $CHCl_3$) within the porous framework.

Results and Discussion

Synthesis of DMOF-1-NH_2 and UMCM-1-NH_2: Utility of NH_2−BDC as a Building Block for Modifiable MOFs. DMOF-1 (DABCO MOF-1) represents a prototypal example of the well-known jungle gym type three-dimensional MOF.[69,70,73,74,76−83] The basic structure contains two-dimensional square grids based on $Zn_2(RCO_2)_4$ paddle-wheel SBUs, which are bridged by BDC at the equatorial positions and pillared by DABCO (1,4-diazabicyclo[2.2.2]octane) at the axial positions. Replacing BDC with NH_2−BDC and following reported procedures[69,70] (with minor modifications) readily generates crystalline products of an isostructural lattice, namely, DMOF-1-NH_2, which can be formulated as $Zn_2(NH_2-BDC)_2(DABCO)$ in its guest-free form. DMOF-1-NH_2 has been characterized by several techniques, including X-ray diffraction, TGA, gas adsorption, ^{1}H NMR, and ESI-MS. Although the atomic coordinates of DMOF-1-NH_2 structure are not currently available from single-crystal X-ray diffraction (because of the poor quality of the diffraction), its phase identity and purity were reliably confirmed by

(76) Seki, K.; Takamizawa, S.; Mori, W. *Chem. Lett.* **2001**, 332–333.
(77) Seki, K. *Chem. Commun.* **2001**, 1496–1497.
(78) Seki, K.; Mori, W. *J. Phys. Chem. B* **2002**, *106*, 1380–1385.
(79) Chun, H.; Dybtsev, D. N.; Kim, H.; Kim, K. *Chem.—Eur. J.* **2005**, *11*, 3521–3529.
(80) Tanaka, D.; Horike, S.; Kitagawa, S.; Ohba, M.; Hasegawa, M.; Ozawa, Y.; Toriumi, K. *Chem. Commun.* **2007**, 3142–3144.
(81) Uemura, K.; Yamasaki, Y.; Komagawa, Y.; Tanaka, K.; Kita, H. *Angew. Chem., Int. Ed.* **2007**, *46*, 6662–6665.
(82) Takei, T.; Ii, T.; Kawashima, J.; Ohmura, T.; Ichikawa, M.; Hosoe, M.; Shinya, Y.; Kanoya, I.; Mori, W. *Chem. Lett.* **2007**, *36*, 1136–1137.
(83) Liu, J.; Lee, J. Y.; Pan, L.; Obermyer, R. T.; Simizu, S.; Zande, B.; Li, J.; Sankar, S. G.; Johnson, J. K. *J. Phys. Chem. C* **2008**, *112*, 2911–2917.

Table 1. Structure Determination Parameters and Mass Spectrometry Data for UMCM-1-NH_2 and UMCM-1-AM5 Single Crystals

MOF	UMCM-1-NH_2	UMCM-1-AM5
formula	$C_{44}H_{25}NO_{13}Zn_4$	$C_{49.50}H_{34.30}NO_{13.90}Zn_4$[a]
morphology	Needle	Needle
color	Beige	Beige
size (mm)	0.38	0.55
	0.15	0.25
	0.14	0.20
crystal system	hexagonal	hexagonal
space group	*P*6(3)/*m*	*P*6(3)/*m*
$a = b$, c	41.2555(8) Å, 17.5091(9) Å	41.2685(10) Å, 17.5342(11) Å
$\alpha = \beta$, γ	90°, 120°	90°, 120°
volume (Å^3)	25808.2(15)	25861.5(18)
T, K	200(2)	200(2)
reflns measured	11730	64158
data/restraints/parameters	3967/0/217	15699/0/306
independent reflns [*R*(int)]	3967[*R*(int) =0.0660]	15699[*R*(int) = 0.2054]
final *R* indices [$I > 2\sigma(I)$][a]	*R*1 =0.0584	*R*1 = 0.0711
	*wR*2 = 0.1587	*wR*2 = 0.1471
R indices (all data, F^2 refinement)[a]	*R*1 = 0.0677	*R*1 = 0.1369
	*wR*2 = 0.1648	*wR*2 = 0.1643
GOF on F^2	0.995	0.786
largest diff. peak and hole, e/Å^3	0.574 and −0.798	0.541 and −1.747
ESI-MS(-) $[M - H]^-$	180	278

[a] The empirical formulas reflect the ratio of unmodified amino-BDC to modified alkyl amide BDC ligand as determined by ^{1}H NMR.

preliminary diffraction data, which provided cell parameter information. The available diffraction data gives a tetragonal cell setting similar to that of DMOF-1 (Supporting Information, Table S1).[69,70] The PXRD pattern for DMOF-1-NH_2 is in good agreement with that of DMOF-1 (Figure 1), which further supports the structural assignment. The mismatch between the simulated (green) and experimental (blue and red) patterns is possibly due to the framework flexibility typically seen in this family of MOFs.[69,81] The dinitrogen sorption isotherms for DMOF-1-NH_2 are also consistent with the expected porosity for this material. The measured BET surface area for DMOF-1-NH_2 is ∼1510 m^2/g with a median pore width of 5.58 Å (calculated from N_2 isotherms at 77 K based on the Horvath−Kawazoe model), which is comparable to, but expectedly lower than, that of DMOF-1 (the reported BET surface area of DMOF-1 range from 1450[69] to 1794 m^2/g;[70] Supporting Information, Figure S1). This shows that DMOF-1-NH_2 is clearly a highly microporous material, with a large surface area, consistent with an open MOF lattice. TGA experiments show that DMOF-1 and DMOF-1-NH_2 decompose in the range of ∼300−350 °C (Supporting Information, Figure S2), which clearly distinguishes them from other MOF materials such as IRMOF-3 (which has a decomposition temperature nearly 100 °C higher).[57,68] In addition, ^{1}H NMR and ESI-MS from the digested DMOF-1-NH_2 samples show the presence of NH_2−BDC and DABCO in the expected relative concentrations for DMOF-1-NH_2 (∼1:0.6 as calculated from ^{1}H NMR integration, Supporting Information, Figure S3; expected value: 1:0.5). All of the aforementioned data support the hypothesis that DMOF-1-NH_2 is an analogue of DMOF-1 with NH_2−BDC present as a surrogate for BDC.

The synthesis of UMCM-1-NH_2 was modified from the published procedure of UMCM-1, a highly porous MOF reported by Matzger et al., which consists of both 1,4-benzenedicarboxylate and BTB linkers.[71] Matzger et al. found UMCM-1 could be synthesized as a single phase crystalline material by controlling the ratio of BDC/BTB within the range of 3:2 to 1:1. We decided to substitute BDC with NH_2−BDC and attempted to synthesize an analogue of UMCM-1. After adjusting the ratio of reagents and reaction conditions from the original UMCM-1 procedure (see Experimental Methods), we were able to synthesize UMCM-1-NH_2 as a single phase material consisting of pale beige crystalline needles. In this case, we found an excess of NH_2−BDC (greater than 2 equiv) was necessary to avoid forming MOF-177.[31]

To confirm UMCM-1-NH_2 was the amino-containing analogue of UMCM-1, UMCM-1-NH_2 was analyzed by ^{1}H NMR, TGA, and PXRD. MOFs of similar ligand compositions (e.g., IRMOF-3, MOF-177, UMCM-1) were also synthesized and examined as standards for direct comparison. UMCM-1-NH_2 was visually identical to UMCM-1 and clearly distinct in color and morphology from IRMOF-3 and MOF-177. Comparison of the ^{1}H NMR spectra of digested samples confirmed the composition of UMCM-1-NH_2 (Supporting Information, Figure S4), showing the expected 2:1 ratio of BTB to NH_2−BDC to be present in UMCM-1-NH_2. TGA and PXRD analysis of UMCM-1-NH_2 were also consistent with those reported for UMCM-1. UMCM-1-NH_2 was observed to have comparable thermal stability (∼450 °C) and showed a similar PXRD pattern to UMCM-1 (Supporting Information, Figure S5).

Unambiguous assignment for the structure of UMCM-1-NH_2 was obtained by a single-crystal X-ray diffraction study. The original UMCM-1 lattice was found to be hexagonal (*P*6$_3$/*m*) with $a = b = 41.5262(8)$ Å, $c = 17.4916(5)$ Å and a unit cell volume of 26129 Å^3.[71] UMCM-1-NH_2 was found to crystallize with the same unit cell parameters as UMCM-1 (Table 1). Suitable atomic positions were found and assigned for three Zn^{2+} ions, 31 carbon atoms, and 8 oxygen atoms in the asymmetric unit (Supporting Information, Figure S6). The atoms present in the asymmetric unit were associated with the Zn_4O cluster, three BTB ligands, and an NH_2−BDC ligand. Unfortunately, a suitable position for the amino group could not be located because of a combination of disorder

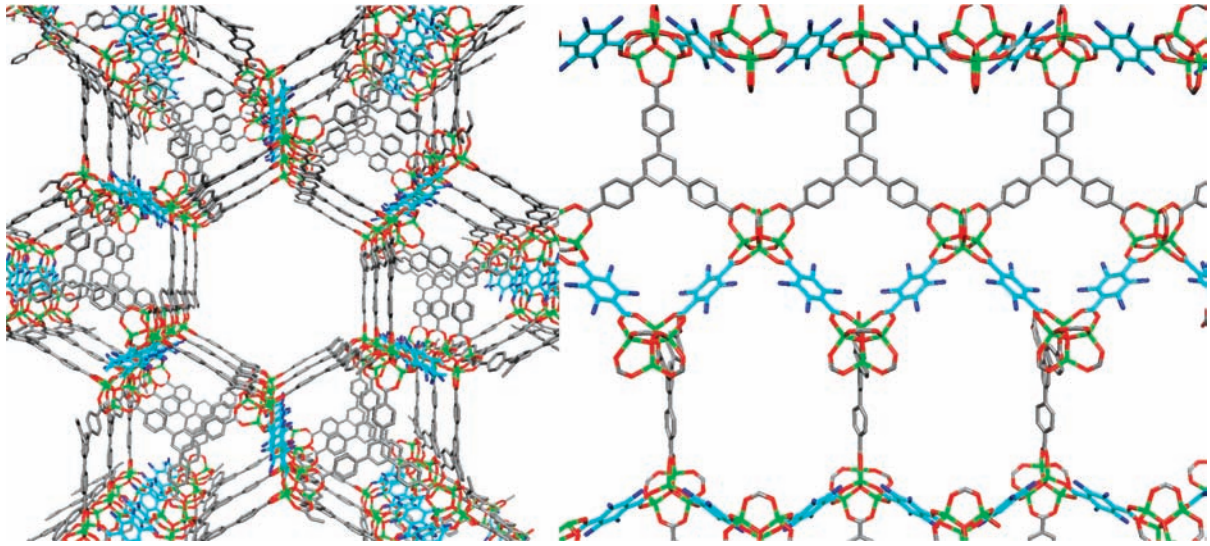

Figure 2. Structure of UMCM-1-NH_2 determined by single-crystal X-ray diffraction (two views). Color scheme: green, Zn; red, O; gray, C; blue, N. Amino groups have been modeled in all four possible positions of the NH_2−BDC ring but were not found in the difference map. The NH_2−BDC ligands are highlighted in cyan.

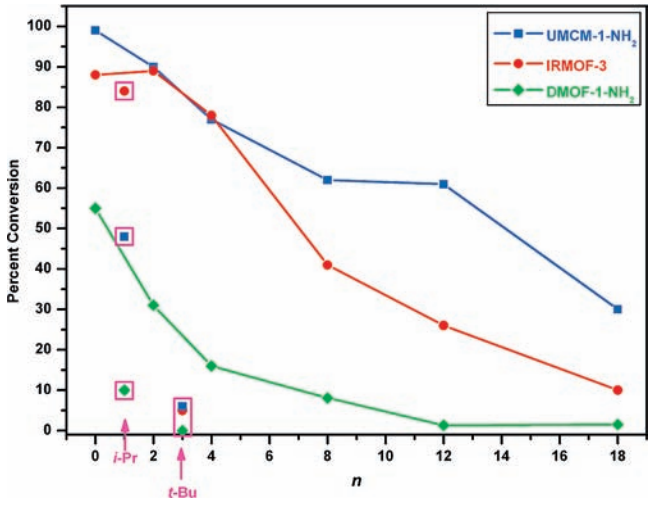

Figure 3. Plots of percent conversion vs length of linear anhydrides (*n*) for IRMOF-3 (red), DMOF-1-NH_2 (green), and UMCM-1-NH_2 (blue) based on Method 1. Data for trimethylacetic anhydride and isobutyric anhydride are also included for comparison.

over four positions of the phenyl ring and the weak diffraction quality of the crystal;[21,57,59] however, ESI-MS and ^{1}H NMR data confirm that the ligands present in these crystals are BTB and NH_2−BDC. UMCM-1-NH_2 is a 3-D extended framework consisting of large 1-D hexagonal channels (Figure 2) bordered by the BTB ligands and smaller pores constructed from a combination of six NH_2−BDC and five BTB linkers, identical to that found for UMCM-1. To confirm the porosity of UMCM-1-NH_2 dinitrogen gas sorption experiments were performed. UMCM-1-NH_2 was found to have a BET surface area of 3973 m^2/g, which is quite comparable to UMCM-1 with a reported BET of 4160 m^2/g. UMCM-1-NH_2 also displayed a characteristic two-step isotherm similar to that of UMCM-1 (vide infra, Figure 5).[71] The high BET surface area and structural analysis of UMCM-1-NH_2 showed unambiguously that NH_2−BDC could act as a substitute for BDC to generate an analogous MOF that is amenable to postsynthetic modification (vide infra).

The facile syntheses of DMOF-1-NH_2 and UMCM-1-NH_2, both of which contain free amino groups within their frameworks, highlight the applicability of using NH_2−BDC as a building block to generate prefunctionalized MOFs suitable for further modification. Although amino groups are known to coordinate to a range of metal ions, our results suggest that their relatively weak binding affinity with Zn^{2+} and small steric hindrance allow the direct replacement of BDC with NH_2−BDC in some systems, without compromising the original MOF structure.[84] The factors that prevent the amino groups from interfering with formation of the desired MOF structure likely lies in the choice of appropriate reaction conditions (e.g., solvent, concentration, temperature, etc.) that disfavor the binding of these groups to metal ions. Considering the large number of BDC-based MOFs in the literature,[85] it is expected that NH_2−BDC can serve as a module to generate a wide range of MOF structures that are suitable for postsynthetic modification. Furthermore, we anticipate the potential accessibility of other amine-containing carboxylate ligands will make this modular approach applicable in an even broader context.

Modification of IRMOF-3, DMOF-1-NH_2, and UMCM-1-NH_2: Influence of Framework Structure on Reactivity. With two new amine-bearing MOFs in hand, a systematic study to functionalize these materials was performed. Specifically, IRMOF-3, DMOF-1-NH_2, and UMCM-1-NH_2, which all possess distinct framework topologies and differing levels of porosity, were used as a basis set to evaluate the effects of structural variation and pore dimension on postsynthetic modification. Eight reagents, including six linear alkyl anhydrides ($[CH_3(CH_2)_nCO]_2O$, where n = 0, 2, 4, 8, 12, 18; corresponding modified products designated as MOF-1 AM1, 3, 5, 9, 13, 19, respectively) and two branched anhydrides (trimethylacetic anhydride and isobutyric anhydride; corresponding to the modified products designated as

(84) Bauer, S.; Serre, C.; Devic, T.; Horcajada, P.; Marrot, J.; Férey, G.; Stock, N. *Inorg. Chem.* **2008**, *47*, 7568–7576.
(85) The Cambridge Structural Database (CSD), ConQuest version 1.10.

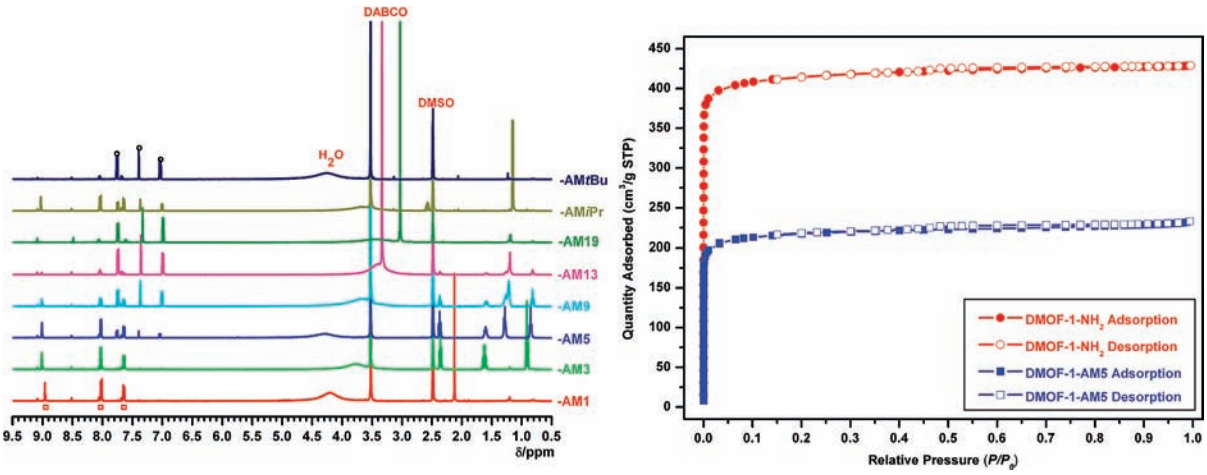

Figure 4. ^{1}H NMR spectra of modified DMOF-1-NH_2 samples digested in DCl/D_2O and DMSO-d_6 (left). Red squares and black circles represent signals of modified and unmodified NH_2−BDC, respectively. N_2 isotherms of DMOF-1-NH_2 and DMOF-1-AM5 at 77 K (right).

Table 2. Percent Conversions of Postsynthetic Modification Reactions with IRMOF-3, DMOF-1-NH_2, and UMCM-1-NH_2 with Different Anhydrides As Determined by ^{1}H NMR[a]

MOF		-AM1	-AM3	-AM5	-AM9	-AM13	-AM19	-AM*i*Pr	-AM*t*Bu
n =		0	2	4	8	12	18	n/a	n/a
Method 1	DMOF-1	55 ± 13%	31 ± 3%	17 ± 3%	8 ± 3%	∼1%	∼1%	10 ± 2%	0%
	IRMOF-3	88 ± 3%	89 ± 6%	78 ± 2%	41 ± 1%	26 ± 3%	10 ± 3%	84 ± 5%	5 ± 1%
	UMCM-1	∼99%	90 ± 5%	77 ± 5%	62 ± 4%	61 ± 3%	30 ± 2%	48 ± 9%	6 ± 3%
Method 2	DMOF-1	∼99%	∼99%	67 ± 3%	34 ± 4%	11 ± 2%	∼2%	63 ± 9%	∼1%
	IRMOF-3[b]	∼99%	∼99%	96 ± 3%	46 ± 7%	32 ± 5%	7 ± 1%	n.d.[c]	n.d.[c]
	UMCM-1	∼99%	∼99%	93 ± 1%	89 ± 5%	84 ± 7%	28 ± 4%	49 ± 4%	∼1%

[a] Values are given for reactions performed under identical (Method 1) and MOF-specific, optimized (Method 2) conditions. Values listed are an average (with standard deviations) of at least three independent experiments. [b] from reference 59. [c] Not determined.

MOF-1-AM*t*Bu, -AM*i*Pr, respectively), were used as amide-coupling reagents to target the amino groups present in the MOFs (Scheme 1). This in turn offered an opportunity to probe another important aspect of this study, to examine how the size and shape of organic reagents will affect the heterogeneous modification process. Strictly identical modification conditions, based on Method 1 as described in the Experimental Section, were applied to all three MOFs. After the reactions were complete, the modified products were handled identically with extensive washing and drying before digested in DCl/D_2O/DMSO-d_6 solutions.

^{1}H NMR taken on the digested samples reveal several interesting observations. First, similar to IRMOF-3,[57,59] both DMOF-1-NH_2 and UMCM-1-NH_2 undergo modification with the anhydrides, corroborating the generality of covalent modification of MOFs.[29,57−61,64,65] Second, under identical modification conditions (i.e., Method 1), percent conversion appears to bear a strong correlation with the nature of the anhydride and the MOF. Overall, UMCM-1-NH_2 tends to have the highest degree of modification (with one notable exception, vide infra), whereas DMOF-1-NH_2 has the lowest and IRMOF-3 lies in between (Figure 3; Table 2). This is in good agreement with their respective surface areas and pore dimensions, with UMCM-1-NH_2 being the most highly porous of the three materials. For the shorter, linear anhydrides ($n \leq 4$) the differences in reactivity between UMCM-1-NH_2 and IRMOF-3 are small. For all three MOFs the percent conversion is found to be inversely related to the length of anhydride, consistent with our previous study.[59] Interestingly, the shape of organic reagent also imposes an influence on the outcome of the modification reaction. For example, trimethylacetic anhydride, the bulkiest reagent used, results in very low conversions (<10%) for all three MOFs. In contrast, isobutyric anhydride, a less bulky reagent, shows drastically different results for the three frameworks, with a conversion as high as 84% for IRMOF-3 and as low as 10% for DMOF-1-NH_2. Surprisingly, isobutyric anhydride shows intermediate reactivity with UMCM-1-NH_2, with a 48% conversion, which is distinct when compared to the trend observed for the linear anhydrides. In all cases, modification was confirmed by ESI-MS analysis by digestion of modified crystals, which showed the presence of the expected m/z peak for the modified NH_2−BDC ligand.

Modification of DMOF-1-NH_2 and UMCM-1-NH_2: Optimization of Reaction Conditions and Characterization of New MOFs. The relatively low conversion for DMOF-1-NH_2 samples modified based on Method 1 suggested that optimization of reaction conditions was necessary to achieve a higher degree of modification. Consequently, the effect of reaction temperatures was initially probed and preliminary results with acetic anhydride (where $n = 0$) suggested that applying heat, even at only slightly higher temperatures (55 °C) dramatically increased the percent conversion (Table 2). Using heat, plus daily rinsing of DMOF-1-NH_2 crystals with $CHCl_3$ and exchange of fresh anhydride solutions,[59] led to the optimal modification conditions for DMOF-1-NH_2 crystals, which resulted in higher conversions and maintained a high degree of crystallinity. The degree of modification was quantified by solution ^{1}H NMR technique (where the modified product was digested

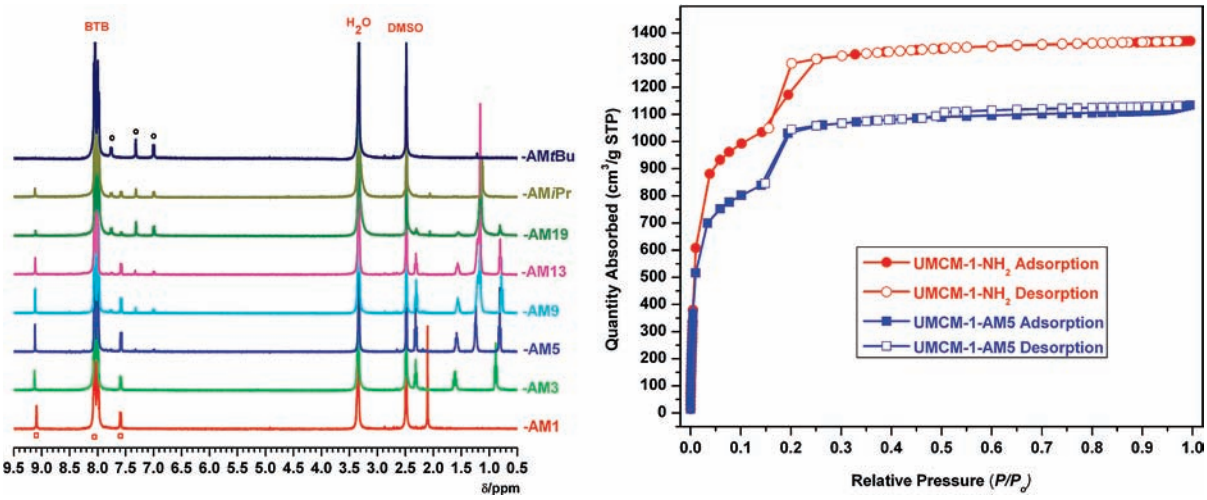

Figure 5. ^{1}H NMR spectra of modified UMCM-1-NH_2 samples (Method 2) digested in DCl/D_2O and DMSO-d_6 (left). Red squares and black circles represent signals of modified and unmodified NH_2−BDC, respectively. N_2 isotherms of UMCM-1-NH_2 and UMCM-1-AM5 at 77 K (right).

in a DCl/D_2O/DMSO-d_6 solution), which revealed a significantly improved percent conversion for most of the smaller anhydrides (Figure 4). In particular, DMOF-1-AM1 and -AM3 were isolated in a nearly quantitatively converted form, whereas -AM5, -AM9, and -AM*i*Pr all showed much higher modification (relative to Method 1). However, the degree of transformation for DMOF-1-AM13, -AM19, and -AM*t*Bu remained notably low, presumably because of the inherent difficulty associated with accommodating these bulkier substituents by the DMOF-1-NH_2 lattice. The structural integrity of the modified DMOF-1-NH_2 samples was corroborated by a number of techniques, including optical microscopy, TGA, PXRD, and gas sorption experiments. As gauged by the images taken on the modified products (Supporting Information, Figures S7), no apparent degradation of the crystals was observed after the reactions, highlighting the expected chemical stability of the DMOF system.[69,70] TGA profiles of these new materials indicated that their thermal stability was essentially retained regardless of modification. The overall structural integrity of the modified DMOF-1-NH_2 crystals was further confirmed by PXRD, which showed good agreement between the most intense reflections of the unmodified and modified DMOF-1-NH_2 samples (Supporting Information, Figure S8). Finally, the porous structures of the eight modified MOFs were also probed using N_2 isotherms measured at 77 K. In general, these new materials all showed a certain degree of microporosity, although their BET surface areas varied widely depending upon the type of substituents and the extent of modification (Supporting Information, Table S2). As a representative example, the N_2 isotherm of DMOF-1-AM5 is shown along with that of unmodified DMOF-1-NH_2, which revealed type I sorption behavior typically seen in microporous materials (Figure 4). The calculated BET surface area for DMOF-1-AM5 was estimated to be about ∼740 m^2/g, and the median pore width to be 5.35 Å based on the Horvath−Kawazoe model. These two values are expectedly lower than those of the unmodified DMOF-1-NH_2 (1510 m^2/g and 5.58 Å, respectively).

To increase the percent modification of UMCM-1-NH_2 with longer, linear anhydrides, a higher anhydride concentration was employed than used in Method 1. Although higher anhydride concentrations were found to partially degrade the single crystallinity of IRMOF-3,[59] the single crystallinity of UMCM-1-NH_2 remained unchanged under these condition (Supporting Information, Figures S9). With higher anhydride concentrations (0.2 M, 8 equiv of anhydride), percent conversions were found to be >80% (n = 2, 4, 8, 12) (Figure 5). Percent conversions for -AM1 and -AM19 remained the same (∼99% for n = 0 and ∼28% for n = 18) as reported for Method 1. UMCM-1-AM5, -AM9, and AM13 were found to have overall percent increases of 20% from the values obtained using Method 1. Improvements in percent conversions with the branched anhydrides were less significant. UMCM-1-AM*t*Bu was ∼1% modified and no significant change was observed with UMCM-1-AM*i*Pr (∼49%). Out of the eight modified versions of UMCM-1-NH_2, UMCM-1-AM9 and -AM13 showed the largest increases in modification in comparison with modified single crystalline IRMOF-3.

All modified UMCM-1-NH_2 were found to maintain thermal and structural stability after anhydride treatment by Method 2. Each modified UMCM-1-NH_2 remained stable up to ∼450 °C (Supporting Information, Figure S8). PXRD data of modified UMCM-1-NH_2 showed peaks consistent with UMCM-1-NH_2 (Supporting Information, Figure S10). To further confirm the structural integrity of the framework, a single crystal X-ray structure was collected and solved for UMCM-1-AM5. Prior to X-ray analysis, UMCM-1-AM5 was determined to be 93% modified by ^{1}H NMR and showed no visual degradation or change in morphology. UMCM-1-AM5 was found to have similar unit cell parameters as UMCM-1-NH_2 (Table 1). Three Zn^{2+} ions, 29 carbon atoms, and 8 oxygen atoms were located and assigned in the asymmetric unit and were found to correspond with the Zn_4O cluster, three BTB ligands, and one modified NH_2−BDC ligand. Suitable atomic positions could not be located for the modified

alkyl-amide substituent because of disorder over four positions of the phenyl ring and because of the weak diffraction quality of the crystal. UMCM-1-AM5 shows the expect framework structure (Supporting Information, Figure S11), identical to that of UMCM-1 and UMCM-1-NH_2, thus indicating UMCM-1-AM5 was structurally intact after modification. After collecting the structure, the UMCM-1-AM5 single crystal was taken from the diffractometer, digested by sonication in MeOH, and submitted for ESI-MS analysis. The expected peak for the modified NH_2−BDC ligand at *m*/*z* 278 $[M - H]^-$ was observed as the base peak in the spectrum (Supporting Information, Figure S12).

BET surface area measurements were collected for the modified UMCM-1-NH_2 to examine the effect of modification on porosity. Two BET trials were collected and averaged for each of the eight modified UMCM-1-NH_2 under dinitrogen at 77 K. All modified UMCM-1-NH_2 were found to remain highly microporous. UMCM-1-AM13 was observed to have the lowest BET surface area (∼2800 m^2/g); consistent with the additional ∼13 non-hydrogen atoms per secondary building unit (i.e., $Zn_4O(RCOO)_6$) having been introduced into the framework.[59] UMCM-1-AM*t*Bu was found to have a BET surface area of ∼3800 m^2/g, essentially unchanged from UMCM-1-NH_2, confirming the low degree of conversion for this material. One interesting observation is that for all of the modified UMCM-1-NH_2 samples, the lowest measured BET is ∼2800 m^2/g. This value is still very high, in excess of many highly porous MOF materials such as IRMOF-3.[21,59,68] Of the two types of pores present in UMCM-1-NH_2, the smaller pore is more likely to be occupied by the substituents generated upon postsynthetic modification because it is the smaller pores that are lined by NH_2−BDC ligands. The large, 1-D hexagonal pores/channels in UMCM-1-NH_2 may remain largely unoccupied, as they are bordered solely by BTB ligands, thus providing these materials with large surface areas even after postsynthetic modification. This hypothesis is supported by a full isotherm collected on UMCM-1-AM5 and its high BET of ∼3300 m^2/g (Figure 5).

Rationale for Modification Results. When identical sets of modification conditions were applied to all three MOFs (i.e., Method 1), the results can be rationalized by considering two key steps involved in the heterogeneous modification process: the *diffusion of reagents* and the *reaction with substitutents*, both of which are related to the kinetics and thermodynamics of postsynthetic modification. In general, a higher surface area, and in particular, larger pore dimension of the MOF should facilitate faster diffusion and easier accommodation of substituents because of reduced steric hindrance. The overall trend of percent conversion observed (UMCM-1-NH_2 > IRMOF-3 > DMOF-1-NH_2) is consistent with this assumption. The negligible difference between UMCM-1-NH_2 and IRMOF-3 for short, linear anhydrides is also consistent with this premise, because both MOFs have highly open structures that readily allow the introduction of small reagents. The extremely low conversion seen in the case of trimethylacetic anhydride with all three MOFs is largely attributed to the low reactivity of this bulky anhydride. In addition to surface area and pore dimension, framework connectivity also influences the covalent transformation of MOFs. In particular, the local environment of the NH_2−BDC ligands (i.e., the amount of free space immediately surrounding the amino groups) may also play an important role in modulating the modification process. This effect is likely to be critical in the modification of DMOF-1-NH_2. Specifically, the plausible edge-to-edge orientation of NH_2−BDC rings (Supporting Information, Figure S13), which places one NH_2−BDC moiety in close proximity to another, potentially limits the accessibility of amino groups to anhydride molecules, thus resulting in significantly lower percent conversions, when compared with UMCM-1-NH_2 and IRMOF-3, even for smaller reagents. This speculation is further supported by the results based on Method 2, where DMOF-1-NH_2 was heated to 55 °C during postsynthetic modification, presumably facilitating free rotation of the NH_2−BDC rings, and resulting in a dramatic increase in the degree of modification by smaller reagents. The unexpected discrepancy of percent conversion for isobutyric anhydride-modified UMCM-1-NH_2 and IRMOF-3 can be explained on a similar basis. UMCM-1-AM*i*Pr was observed to have lower conversion than IRMOF-3-AM*i*Pr under identical reaction conditions (Method 1). While higher anhydride concentrations appeared to improve the percent modification of the linear alkyl chains, use of a higher anhydride concentration had no effect on the formation of UMCM-1-AM*i*Pr, which may be due to the shape and sterics of the branched substituent. Although UMCM-1-NH_2 has a significantly higher overall porosity than IRMOF-3, examination of their structural models suggests that the size of local channels and cavities adjacent to amino moieties in UMCM-1-NH_2 are smaller than that in IRMOF-3 (Supporting Information, Figure S13), the effect of which appears to be more pronounced for branched anhydrides than for their linear counterparts.

Conclusions

Robson suggested with the very earliest MOF-like materials that postsynthetic modification would be a promising route toward preparing novel materials with interesting properties. Herein, our controlled modification performed on the three structurally diverse MOFs has identified several key concepts that are of particular importance in the process of postsynthetic modification: (1) overall porosity of MOFs largely determines the degree of modification and the range of reagents that can be accessed; (2) framework connectivity and in particular, local environment surrounding the targeted reactive groups (e.g., NH_2) play an important role that affects the reactivity; and, (3) the size and shape of reagent molecules also play a critical role in influencing the modification outcome. We believe these conclusions are of general importance and can serve as guidelines for the postsynthetic modification of other MOF systems. In addition, we have also demonstrated the feasibility of modulating known BDC-based MOF structures with NH_2−BDC units, which affords an easy handle for postsynthetic modification

targeting the reactive amino groups. We anticipate this approach to be applicable in a broader context, as other amine-containing MOFs are also potentially accessible. Together, we believe this work provides a validated, conceptual framework for the general application of postsynthetic modification to MOFs.

Acknowledgment. We thank Dr. J. R. Stork for help with X-ray analyses, Prof. G. Arrhenius for use of his PXRD, and Dr. Y. Su for performing the mass spectrometry experiments. This work was supported by UCSD and the NSF (CHE-0546531).

Supporting Information Available: Further details are given in Figures S1−S13, Tables S1−S3, and crystallographic data in CIF format. This material is available free of charge via the Internet at http://pubs.acs.org.

IC801837T